ELSEVIER

Ceramics International 33 (2007) 789–793

CERAMICS INTERNATIONAL

www.elsevier.com/locate/ceramint

R-curve behavior of Ti_3SiC_2

Debasish Sarkar [a], Bikramjit Basu [b,*], Min Cheol Chu [c], Seong Jai Cho [c]

[a] Department of Ceramic Engineering, National Institute of Technology, Rourkela-769008, Orissa, India
[b] Department of Materials and Metallurgical Engineering, Indian Institute of Technology, Kanpur 208016, India
[c] Department of Materials Evaluation Center, Korea Research Institute of Science and Standards, Daejeon 305-600, Korea

Received 17 October 2005; received in revised form 15 November 2005; accepted 30 January 2006
Available online 18 April 2006

Abstract

One of the characteristic material properties for many of the high toughness ceramics (ZrO_2, Sialon, etc.) is the enhanced resistance to crack growth during crack extension, a phenomenon known as 'R-curve behavior'. Herein, we report, the crack growth resistance/R-curve behavior of Ti_3SiC_2. The crack growth resistance property of Ti_3SiC_2 is experimentally measured using single-edge-precrack-notched beam (SEPB) method. At room temperature, the flexural tests of hot pressed Ti_3SiC_2 bars are performed under 4-point bending mode and the precrack length is varied in our experiments. Additionally, the fracture toughness/crack growth resistance behavior as well as fracture mechanisms of Ti_3SiC_2 are explained on the basis of microstructure and bonding in Ti_3SiC_2. SEM investigation reveals significant crack wake bridging, which is a characteristic feature of many high toughness damage-tolerant ceramic.

Keywords: Ti_3SiC_2; SEPB; R-curve

1. Introduction

It has been widely recognized that a major limitation of ceramics for various structural applications is the brittleness, i.e., poor fracture toughness [1]. This has motivated researchers to develop toughened ceramics either by composite/laminate approach or by engineering the composition/microstructure of ceramic monoliths [2]. One of the characteristic features exhibited by many of the toughened ceramics/ceramic composites is the 'Resistance/R-curve' behavior [2]. Fig. 1 illustrates the typical R-curve behavior exhibited by a toughened ceramic material. In Fig. 1, the length of the V-notch is symbolized as '*n*', which is constant for all of the specimens. It can also be noted that a well defined bridging/process zone develops around the growing crack [3]. Under 4-point bending, an increase in the length of this precrack zone diminishes the driving force at the crack tip, i.e., an increase in macroscopic crack resistance is expected with the extension of crack. Further crack propagation from the crack tip occurs until steady-state toughness (K_{ss}) is reached. In a recent study, Mattoni and Zok critically analysed the mechanics and phenomenology of R-curve behavior in ceramic composites [4]. The toughness properties in terms of R-curve behavior are studied for Si_3N_4 ceramics [5] and the observation of a threshold stress intensity factor for the onset of a stable crack growth is reported by Lube and Fett [6]. In a theoretical study, the effect of notch geometry, in particular notch route radius, on the R-curve response is analyzed by Fett [7]. From his theoretical analysis, one can infer that the R-curve behavior is solely controlled by the development of process zone around the crack and the precrack length does not have any significant influence. Herein, we report the R-curve behavior of another interesting ceramic material, i.e., Ti_3SiC_2.

In last two decades, the research on ternary carbides like Ti_3SiC_2 is triggered mainly by Barsoum and co-workers [8–11]. Ti_3SiC_2 has layered structure with high *c*/*a* ratio of typically around 6–8. The major properties of Ti_3SiC_2 include excellent resistance to oxidation up to 1400 °C, high thermal shock resistance, high elastic modulus (325 GPa), relatively low hardness (4–5 GPa) and good machinability with conventional tools [8]. Because of interesting property combination, the mechanical behavior of Ti_3SiC_2 was investigated with a focus to understand the structure-property correlation. In a recent research article, Zhen et al. [12] reported the results of an

* Corresponding author. Tel.: +91 512 2597771; fax: +91 512 2597505.
E-mail address: bikram@iitk.ac.in (B. Basu).

0272-8842/$32.00
doi:10.1016/j.ceramint.2006.01.002

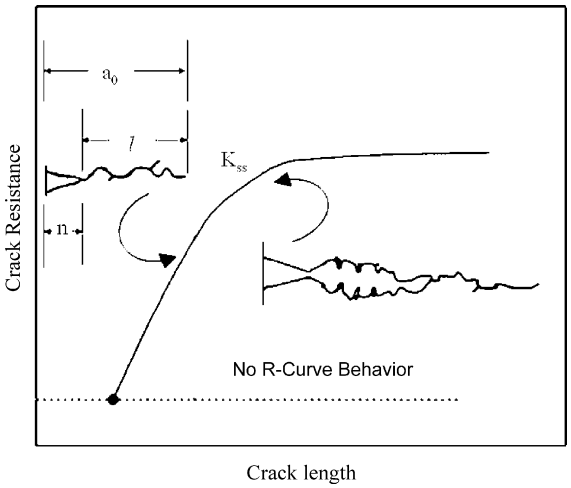

Fig. 1. An ideal representation of the functional dependence of fracture toughness on flaw size for a ceramic exhibiting R-curve (top curve) and one that does not (lower curve). Ceramics exhibiting R-curve behavior are more flaw-tolerant than those that do not. The description of the figure has been made in Section 1.

extensive compressive deformation study conducted on Ti_3SiC_2. In their experiments, the influence of strain rate and temperature (up to 1200 °C) on the cyclic stress–strain response of Ti_3SiC_2 with varying grain size is investigated. The compressive deformation behavior was discussed in terms of dislocation dynamics as well as kink bands. In another interesting work, Sun et al. [13] investigated the mechanical properties of porous Ti_3SiC_2, having 57% density. Uniaxial compression and nanoindentation experiments, conducted at room temperature, reveal the hysteresis stress–strain behavior of porous Ti_3SiC_2. Most importantly, an order of magnitude, higher energy dissipation than the dense Ti_3SiC_2 with comparable grain size was measured in porous Ti_3SiC_2. This was attributed to the easier formation of more kink bands in the presence of pores. Apart from the experimental observation of deformation during compression, Sarkar et al. [14] reported the evidence of plastic deformation process on worn Ti_3SiC_2, after fretting against steel. The influence of load on tribological properties was studied in this work with a focus to understand the mechanism of material removal process from the fretted interface. More extensive discussion on the deformation during tribological interaction is reported in another research paper [15].

The crack resistance curve (R-curve) of ternary carbides has been characterized by only Compact Tension (CT) method (ASTM standard E647), which is complicated and expensive [10]. El-Raghy et al. reported that the fracture toughness of Ti_3SiC_2 can be estimated using single edge notched beam (SENB) method, where notch was made using a diamond wheel with a width of 80 μm and a depth of 500 μm [11]. Usually, in ternary carbides (Ti_3SiC_2), unlike other ceramics, it is difficult to introduce initial flaw by any conventional indentation-bridge loading technique, because of lower hardness and layered structure. In the present work, single-edge-precrack-beam (SEPB) [16] technique has been used, which enables us to introduce a controlled initial flaw and determine the crack resistance curve of Ti_3SiC_2. Finally, an attempt has been made to explain the toughening mechanisms in Ti_3SiC_2.

2. Experimental procedure

Monolithic Ti_3SiC_2 disks were synthesized by hot pressing method. The green compacts containing appropriate stoichiometric amounts of $TiC_{0.67}$ and Si (−325 mesh, 99.99% purity) were hot pressed at 1420 °C for 90 min under Ar atmosphere at 5 MPa pressure to obtain the final density of 98–99% ρ_{th}. The larger disk specimen (Ø 55 mm, height 25 mm) was used to fabricate the specimens for fracture toughness measurement and R-curve determination. The test samples were cut out using diamond blades into the desired sample size (35 mm × 4 mm × 3 mm) from a large hot pressed disc and subsequently polished on 4 mm × 35 mm surface to a 1200 grit finish, followed by polishing steps using a 15 μm diamond suspension and finally 1 μm diamond suspension. Subsequently, the V-notch was introduced on the test sample with a simple machine by 'to and fro' sliding razor blade over the middle of the (3 mm × 35 mm) surface, while impinging 1 μm diamond slurry along the surface of the blade [17]. The notch length was measured by observing the polished surface using an optical microscope (Matsuzawa DVK-2S). The measured average notch length (n) was varied within 0.50–0.55 mm. A sharp precrack was ''popped'' into the beam at room temperature via the bridge–indentation method [18]. Again, the initial precrack length (l) was calculated using optical microscope. The specimen was then aligned with the perpendicular crack exactly in the center of the groove and a flexural load was applied with a 4-point bending arrangement. The mechanical testing was performed on a screw-driven load frame (Model Instron 4465, Instron Corporation, USA) equipped with a 5 kN load cell. The specimens were fractured at room temperature with a 4-point bending fixture with 30 mm outer span and 10 mm inner span and cross head speed of 0.5 mm/min. The fracture load was retrieved and the peak load required to fracture of the specimen was recorded. The mode-I critical stress intensity factor (K_{IC}), a measure of fracture toughness, was calculated from the standard equations [19,20]:

$$K_{IC} = g\frac{P_{max}S}{BW^{3/2}}\frac{3(a/W)^{1/2}}{2(1-a/W)^{3/2}} \quad (1)$$

where

$$g = \frac{1.99-(a/W)(1-a/W)[2.15-3.93(a/W)+2.7(a/W)^2]}{1+2(a/W)} \quad (2)$$

where a = average precrack length, W = thickness of the beam (nominally 4 mm), g = a geometric factor based on the average crack length and specimen thickness, P_{max} = maximum load required for fracture, $S = (S_0 - S_i)$, where outer span length, S_0 = 30 mm and inner span length, S_i = 10 mm, B = width of the beam (nominally 3 mm). It should be noted that Eqs. (1) and (2) are valid for (S/W) ratio of 4–5 and (a/W) ratio varying between 0.35 and 0.70. In the present case, for the given

specimen geometry ($S = 20$ mm and $W = 4$ mm), the Eqs. (1) and (2) can be applied as $(S/W) = 5$ and (a/W) also varies within 0.35 and 0.70.

The polished and fractured (4 mm × 35 mm surface) samples were etched using a 1:1:1 by volume HF:HNO_3:H_2O solution and the microstructural features are observed under scanning electron microscopy. The hot pressed Ti_3SiC_2 microstructure is characterized by platelike elongated grain (∼50–200 μm) with an aspect ratio of ∼8 (not shown). X-ray diffraction analysis also confirmed the predominant presence of Ti_3SiC_2 with a small amount of TiC [14]. The density of the Ti_3SiC_2 flat sample was found to be 4.5 gm/cm^3. The investigated polycrystalline Ti_3SiC_2 has a combination of moderate hardness (∼5 GPa), lower than hardened steel (∼7 GPa), and good fracture toughness (∼9 MPa m$^{1/2}$), better than many structural ceramics (2–5 MPa m$^{1/2}$).

3. Results and discussion

In a first attempt to use indentation technique to measure toughness, Vickers indent on a polished Ti_3SiC_2 is taken at 98 N load. The indented surface is shown in Fig. 2. The indentation could not develop any radial crack from the edges of the Vickers indentation and instead produces considerable material deformation around the indentation zone. This type of indentation behavior is also reported earlier by Pampuch et al. [21]. In another work, delaminations, kinking of individual grains, grain push-outs and pull out have been observed in the area of indentations [22]. We believe that the main reason for this behavior is the ability of the Ti_3SiC_2 to contain and confine the extent of damage to a small area around the indentations due to its laminated and elongated structure. Hence, determination of fracture toughness of Ti_3SiC_2 by measuring radial crack length is impossible, because of its high damage-tolerant property. Therefore, to evaluate the fracture toughness of Ti_3SiC_2 another technique is used, which is known as 'single-edge-precrack-beam method through V-notch approach' [16].

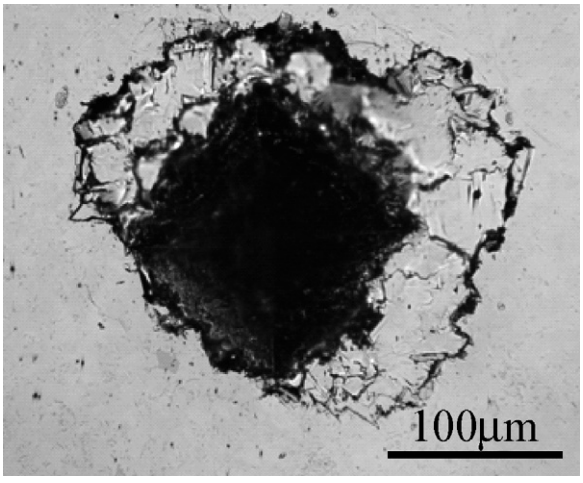

Fig. 2. Optical microscopy image revealing the indented region (Vickers indentation) on a polished Ti_3SiC_2 surface, indented using 10 kg load. Notice the absence of any radial crack from the edges of Vickers indentation.

By varying the precrack length, the crack growth resistance is measured for a series of Ti_3SiC_2 specimens following earlier mentioned Eqs. (1) and (2). The obtained fracture toughness data, average values of at least five specimens, are compiled in Fig. 3. The experimental data, plotted in Fig. 3, displays the characteristic 'R-curve behavior'. It can be noted that while initial $K_R = 5.32$ MPa m$^{1/2}$, it increases steadily with increase in precrack length and reaches to a steady-state crack growth resistance value of 8.98 MPa m$^{1/2}$, when the precrack length is more than 1.25 mm.

In order to analyze the measured 'R-curve' data, we followed a theoretical analysis [23] correlating K_R with crack length parameter:

$$K_R(c) = K_{IO} + A\left[1 - \exp\left\{\frac{-(c - c_0)}{B}\right\}\right] \quad (3)$$

where $K_R(c)$ = crack growth resistance with a particular precrack length (MPa m$^{1/2}$), K_{IO} = fracture toughness without a precrack (MPa m$^{1/2}$), A and B are constants for a particular system with A having unit in MPa $\sqrt{}$m and B in mm, $c_0 = 0$ (initial flaw size, only V-notch, without any precrack length, i.e., 'n'), c = precrack length (l), in mm.

Our experimental data appear to fit the above formulation and the 'R-curve' behavior of investigated Ti_3SiC_2 can be described as;

$$K_R(c) = 5.32 + 3.186\left[1 - \exp\left\{\frac{-(c - c_0)}{0.56}\right\}\right] \quad (4)$$

From the present experimental results, 'R-curve' of Ti_3SiC_2 initiates at 5.32 MPa m$^{1/2}$ and reaches a steady-state behavior at 8.98 MPa m$^{1/2}$, from which it is conceivable that the high initiation toughness value is associated with some degree of residual bridging in the precrack. It should be noted that the initial precrack size appeared to affect the initial toughness, which is manifested as the starting point of the 'R-curve'. This is considered to be associated with residual bridging in the crack during fracture. However, significantly more bridging

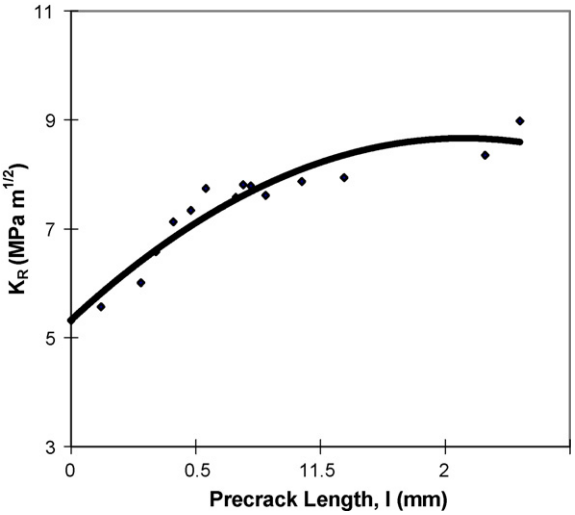

Fig. 3. Room temperature crack resistance curve of Ti_3SiC_2 under 4-point flexural mode of loading. Loading condition is displayed in the inset.

effect is expected in the coarse grained Ti_3SiC_2 structure, which may exhibit higher plateau toughness at ambient temperature [10]. It can be mentioned that, the fracture toughness of Ti_3SiC_2, measured by Compact Tension method was reported to be 9.5 and 16 MPa $m^{1/2}$ for fine (3–10 μm) and coarse (50–200 μm) grain, Ti_3SiC_2, respectively [11].

The fracture mechanism and characteristic R-curve of Ti_3SiC_2 can be explained as follows. Ti_3SiC_2 is characterised by relatively weak bonding between the silicon layer and the TiC octahedra along the basal plane. Usually, the dislocations of Ti_3SiC_2 are mobile and multiply at room temperature [24]. The dislocation movement is restricted to two orthogonal directions: basal plane and walls or kink boundaries. In general, the deformation behavior seen in Ti_3SiC_2 is unusual for carbides and is caused by the layered structure and the metallic nature of the bonding [25]. In addition to regular slip, mechanisms for ambient temperature plastic deformation in Ti_3SiC_2 are thought to involve the readjustment of local stress fields from kink band (boundaries) formation, buckling, and delamination of individual grains [25]. Specifically, delamination along the weaker basal planes leads to the creation of microlaminae contained within a single grain and consequently, the deformation and distortion of such laminae provides a potent contribution to toughening.

The microstructure-crack path interaction reveals that the crack paths are significantly tortuous in nature. As shown in Fig. 4a, when a crack propagates through bulk Ti_3SiC_2, crack deflection occurred along the weak interface continually, leading to a fluctuating crack propagation path, which greatly extended effective crack length and absorbed more fracture energy with an improvement of fracture resistance. SEM image (Fig. 4b) of the fracture surface reveals that the deformed lamellae bridge the crack and distort the crack path. The ligaments shown in Fig. 4b are further examples of the extent by which individual grains of Ti_3SiC_2 can deform. Besides, crack branching and crack delamination appearing at the weak interface, the fracture energy is also absorbed in this physical process. This relaxes the stress at the crack tip and improves the fracture resistance and damage resistance. Such bridging processes are evidences for both elastic-ligament bridging and frictional pullout, similar to bridging processes observed in well-studied systems like Al_2O_3/SiC_w composites [23]. In addition, crack paths involved more transgranular and/or translamellar cracking to a large extent. In particular, this severely diminishes the propensity for grain bridging in the crack wake in the fine-grained (5–20 μm) microstructure. This enhanced crack growth resistance, typically absent in other layered compounds such as mica and graphite, can be traced to the metallic nature of the bonding and the absence of strong in-plane Si–Si bonds in case of Ti_3SiC_2 [24]. This bonding characteristic is highly unusual in ceramic systems and account for the high steady-state fracture toughness by promoting crack bridging.

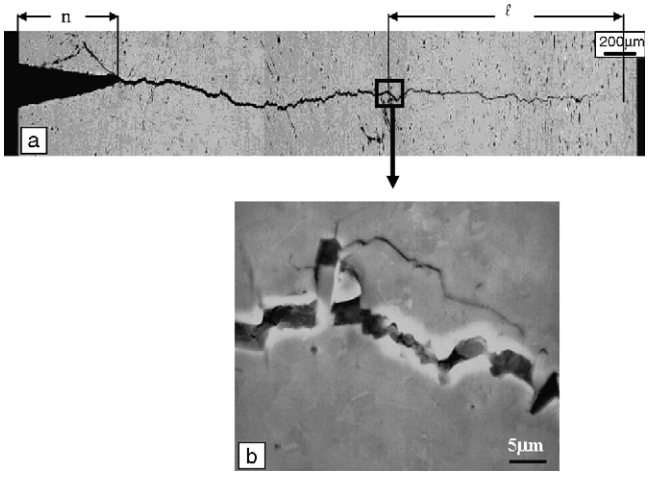

Fig. 4. Optical micrograph revealing the fracture surface after the flexural testing under 4-point bending configuration. The deformed and tortuous nature of precrack is observed at the crack tip (a). SEM image illustrating the crack-wake bridging at the crack tip (b).

4. Conclusions

(a) The crack growth resistance properties of Ti_3SiC_2 are experimentally studied. Under 4-point flexural load, the crack growth resistance property of layered Ti_3SiC_2 displays rising resistance-curve (R-curve) behavior. The initial fracture toughness of Ti_3SiC_2 was recorded to be 5.32 MPa $m^{1/2}$, while with increasing precrack length; the toughness reaches a steady-state value at 8.98 MPa $m^{1/2}$.
(b) The microscopic observations include crack propagation by intergranular and transgranular mode with consequent crack-tip shielding by grain bridging in the crack wake. The initial flaw size dominated the crack propagation mechanism.

Acknowledgement

This research was supported partially by a research grant (code #: M105KO010006-05K1501-00612) from ‘Center for Nanostructured Materials Technology’ under ‘21st Century Frontier R&D Programs’ of the Ministry of Science and Technology, Korea.

References

[1] Y.-M. Chiang, D. Birnie, W.D. Kingery, Physical Ceramics: Principles for Ceramic Science and Engineering, John Wiley & Sons Inc, New York, 1997, pp. 398–404.
[2] B. Basu, Toughening of Y-stabilized tetragonal zirconia ceramics, Int. Mater. Rev. 50 (4) (2005) 239–256.
[3] G.D. Quinn, J. Salem, I. Bar-on, K. Cho, M. Foley, H. Fang, Fracture toughness of advanced ceramics at room temperature, J. Res. Natl. Inst. Stand. Technol. 97 (1992) 579–607.
[4] M.A. Mattoni, F.W. Zok, Notch sensitivity of ceramic composites with rising fracture resistance, J. Am. Ceram. Soc. 87 (5) (2004) 914–922.
[5] C.W. Li, D. Lee, S.C. Lui, R-curve behavior and strength for in-situ-reinforced silicon nitrides with different microstructures, J. Am. Ceram. Soc. 75 (1992) 1777–1785.
[6] T. Lube, T. Fett, A threshold stress intensity factor at the onset of stable crack extension of Knoop indentation cracks, Eng. Fract. Mech. 71 (2004) 2263–2269.
[7] T. Fett, Influence of a finite notch root radius on the measured R-curves, J. Mater. Sci. 39 (9) (2004) 1061–1063.

[8] T. El-Raghy, M.W. Barsoum, Processing and mechanical properties of Ti_3SiC_2: I, reaction path and microstructure evolution, J. Am. Ceram. Soc. 82 (10) (1999) 2849–2854.
[9] T. El-Raghy, A. Zavaliangos, M.W. Barsoum, S.R. Kalidindi, Damage mechanisms around hardness indentations, J. Am. Ceram. Soc. 80 (1997) 513–516.
[10] D. Chen, K. Shirato, M.W. Barsoum, T. El-Raghy, R.O. Ritchie, Cyclic fatigue-crack growth and fracture properties in Ti_3SiC_2 ceramics at elevated temperatures, J. Am. Ceram. Soc. 84 (No. 12) (2001) 2914–2920 (7).
[11] T. El-Raghy, A. Zavaliangos, M.W. Barsoum, S.R. Kalidindi, Damage Mechanisms around Hardness Indentations in Ti_3SiC_2, J. Am. Ceram. Soc. 80 (2) (1997) 513–516.
[12] T. Zhen, M.W. Barsoum, S.R. Kalidindi, Effects of temperature strain rate and grain size on the compressive properties of Ti_3SiC_2, Acta Materialia 53 (15) (2005) 4163–4167.
[13] Z.M. Sun, A. Murugaiah, T. Zhen, A. Zhou, M.W. Barsoum, Microstructure and mechanical properties of porous Ti_3SiC_2, Acta Materialia 53 (16) (2005) 4359–4366.
[14] D. Sarkar, S.J. Cho, M.C. Chu, S.S. Hwang, S.W. Park, B. Basu, Tribological properties of Ti_3SiC_2, J. Am. Ceram. Soc. 88 (11) (2005) 3245–3248.
[15] D. Sarkar, B.V. Manoj Kumar, B. Basu, Understanding the fretting wear of Ti_3SiC_2, J. Eur. Cer. Soc., in press (Corrected Proof Available online 28 July 2005).
[16] Standard test methods for the determination of fracture toughness of advanced ceramics at ambient temperatures, ASTM Provisional Standard Designation No. PS070-97. American Society for Testing and Materials, West Conshohocken, PA.
[17] G. Rauchs, T. Fett, D. Munz, R-curve behaviour of 9Ce-TZP zirconia ceramics, Eng. Fract. Mech. 69 (2002) 389–401.
[18] R. Matt, Statisches und Zyklisches Ermüdungsverhalten Umwandlungsverstärkter ZrO2-Werkstoffe, Dissertation, Universität Karlsruhe, IKM 016, 1996.
[19] H. Tada, The Stress Analysis of Cracks Handbook, second ed., Paris Productions Inc, St Louis, MO, 1985.
[20] Standard test methods for the determination of fracture toughness of advanced ceramics at ambient temperatures, ASTM Provisional Standard Designation No. PS070-97. American Society for Testing and Materials, West Conshohocken, PA.
[21] R. Pampuch, J. Lis, L. Stobierski, M. Tymkiewicz, Solid combustion synthesis of Ti_3SiC_2, J. Eur. Ceram. Soc. 5 (1989) 283.
[22] T. El-Raghy, A. Zavaliangos, M.W. Barsoum, S. Kalidinidi, Damage mechanisms around hardness indentations in Ti_3SiC_2, J. Am. Ceram. Soc. 80 (1997) 513–516.
[23] B.R. Lawn, Fracture of Brittle solids, second ed., Cambridge University Press, Cambridge, UK, 1998.
[24] M.W. Barsoum, D. Brodkin, T. El-Raghy, Layered machinable ceramics for high temperature applications, Scrip. Met. Mater. 36 (1997) 535–541.
[25] M.W. Barsoum, L. Farber, T. El-Raghy, I. Levin, Dislocations, kink banks and room temperature plasticity of Ti_3SiC_2, Metall. Mater. Trans. A 30 (1999) 1727–1738.